

A 2 to 4 nm HIGH POWER FEL ON THE SLAC LINAC*

C. Pellegrini, J. Rosenzweig
UCLA Department of Physics, Los Angeles, California 90024
H.-D. Nuhn, P. Pianetta, R. Tatchyn, H. Winick
Stanford Synchrotron Radiation Laboratory, Stanford University, Stanford, California 94309
K. Bane, P. Morton, T. Raubenheimer, J. Seeman
Stanford Linear Accelerator Center, Stanford University, Stanford, California 94309
K. Halbach, K.-J. Kim
Lawrence Berkeley Laboratory, Berkeley, California 94720
J. Kirz
State University of New York at Stony Brook, Stony Brook, New York

ABSTRACT

We report the results of preliminary studies of a 2 to 4 nm SASE FEL, using a photoinjector to produce the electron beam, and the SLAC linac to accelerate it to an energy up to 10 GeV. Longitudinal bunch compression is used to increase ten fold the peak current to 2.5 kA, while reducing the bunch length to the subpicosecond range. The saturated output power is in the multi-gigawatt range, producing about 10^{14} coherent photons within a bandwidth of about 0.2% rms, in a pulse of several millijoules. At 120Hz repetition rate the average power is about 1 W. The system is optimized for x-ray microscopy in the water window around 2 to 4 nm, and will permit imaging a biological sample in a single subpicosecond pulse.

1. INTRODUCTION

The Self Amplified Spontaneous Emission mode of an FEL has been proposed [1] and analyzed [2] as a source of tunable, coherent, high peak power soft X-rays, capable of

* Work supported by the US Department of Energy, Offices of Basic Energy Sciences and High Energy Physics, contracts DE-AC03-76SF00098 and DE-AC03-76SF00515.

producing a radiation beam with a brightness eight orders of magnitude larger than synchrotron light sources, and pulse duration shorter than one picosecond. Such a large increase in radiation flux, and the short pulse duration, will open new exciting and unique research possibilities in physics, biology and other sciences.

The SASE approach produces lasing in a single pass of a high peak current electron beam through a long undulator, eliminating the need for optical cavities, difficult to build at these short wavelengths. The requirements on the electron beam peak current, emittance, and energy spread are very stringent [2], and until recently difficult to satisfy. The recent development of high-brightness photocathode electron guns [3], and the expected availability of the SLAC linac, open the possibility to make this major extension of FEL operation, from the shortest wavelength yet achieved (240 nm) to 2-4 nm, the wavelength range suitable for biological imaging and other applications.

The recognition of this possibility was one of the main conclusions of the Workshop on Fourth Generation Light Sources held at SSRL/SLAC on February 24-27, 1992. The workshop report [4] contains many contributions relevant to linac-driven short wavelength FELs. In particular, the use of the SLAC linac for this purpose is discussed by C. Pellegrini [5], K.-J. Kim [6], and by W. Barletta, A. Sessler and L. Yu [7]. The advantage of using the SLAC linac is that its properties are extensively characterized, because of its use as a linear collider [8-12].

The wavelength range 2 to 4 nm, corresponding to the "water window", is most suitable for imaging biological materials and other applications in which the short pulse and high coherent power are important. In particular we consider the use of this system for x-ray microscopy and holography of biological samples, with images obtained in a single pulse [13]. This requires an energy in a single photon pulse of the order of 300 mJ/cm^2 , and a

subpicosecond pulse duration. Under this condition an image is obtained for a sample "in vivo" before it has time to change, or be affected by the radiation.

The system for the 2-4 nm FEL consists of: a 10 MeV, S-band photoinjector; part of the SLAC linac to accelerate the beam up to 10 GeV; two longitudinal bunch compressors, to increase the peak current to 2500 A, and reduce the rms bunch length to 0.16 ps; the undulator; optical beam transport lines and experimental areas. These components will be discussed in the next sections.

It is interesting to notice that, with an improvement of present photocathode gun technology, it appears possible to reduce in the near future the normalized emittance by a factor of about 3 below that used for the 4 nm FEL. This would open the possibility to construct a 0.1 nm FEL using the entire SLAC linac, permitting acceleration up to 55 GeV.

2. THE PHOTOINJECTOR

The electron source is a critical component, since it defines the electron beam properties. The requirements for the 2-4 nm FEL are given in Table 1. A preliminary study indicates that an electron beam of characteristics approaching the design goal can be obtained from an RF photocathode gun. This source consists of a three and a half cell π -mode standing wave accelerating structure, excited to 100MV/m peak field on axis, with a metal photocathode illuminated by a two picosecond laser pulse.

Using a simple analytical model [14], we estimate that for a bunch with radial size $\sigma_r=3$ mm, and longitudinal size $\sigma_z=0.54$ mm, the emittance growth due to the space charge force, is

2.5 mm-mrad. Additional emittance growth due to the time dependent RF field is small, 0.7 mm-mrad, because of the size of the electron beam.

The beam envelope is controlled without additional solenoidal or quadrupole focusing using alternating gradient (ponderomotive) focusing effects [15] of the high gradient RF field.

The normalized, rms, according to Parmela simulation is 6 mm-mrad for a bunch charge of 1 nC. This is larger than the actual emittance obtainable from the source, as numerical noise in the space charge calculation done by Parmela typically inflates the emittance by a factor of two when compared to experimental results and to calculations using particle-in-cell codes. On this basis we assume that the gun will produce the required design value of 3 mm-mrad. Calculations using a particle-in-cell model for our gun are in progress.

The longitudinal phase space has an rms pulse length of $\sigma_l = 0.5$ mm, peak current of 250 A, rms momentum spread 1.8×10^{-3} . The uncorrelated momentum spread which appears towards the rear of the bunch is due to the longitudinal space charge field of the bunch and its image near the cathode.

3. BEAM TRANSPORT, ACCELERATION AND COMPRESSION

We consider the acceleration and compression of the bunch produced by the photoinjector. We initially consider the case of acceleration to 7 GeV, with a longitudinal compression by a factor of 10. At the end of the linac, we require a peak current of 2.5kA and a peak-to-peak energy spread $\Delta_E < 0.2\%$.

In deciding at what energy to compress we need to consider the longitudinal and transverse wakefields and RF deflections in the linac[8-12]. The first will increase the beam's

energy spread and is harder to compensate for short bunches; the last will increase the transverse emittance and are more severe for long bunches. In addition we have to consider the characteristics of the bunch compressors, which limit the compression factor we can expect to achieve in a single stage of compression.

We compress in two stages, once at 70 MeV to achieve the shortest bunch length, 200 μ m, consistent with correcting the correlated energy spread to the level of 0.2%, and again at 7 GeV to 30 μ m, to achieve the desired high peak current. To study the development of longitudinal phase space we use a computer program that considers the effects of both the longitudinal wakefields and the curvature of the RF wave. After the initial compression the beam shape is still very similar to a gaussian. After the second compression, the beam distribution is more sharply spiked and has long tails, as shown in Fig. 1. We note that the peak current and the final energy spread satisfy our requirements.

Next, we calculate the transverse emittance dilution due to the transverse wakefields, rf deflections, and dispersive errors. To model the SLAC linac, we assume 150 μ m rms random misalignments of the quadrupoles and BPMs, 300 μ m rms random misalignments of the accelerator structures, and a random transverse-longitudinal coupling $g_{rms}=2\times 10^{-4}$ for the RF deflections. Finally, we assume a transverse beam jitter equal to the rms beam size. The results, averaged from ten sets of random errors, are plotted in Fig. 2, along with the final peak-to-peak energy spread, as a function of the bunch length in the linac.

The apparent knee in the energy spread occurs because one cannot use the curvature of the RF to fully cancel the longitudinal wakefield for bunches shorter than roughly 200 μ m. At a bunch length of 200 μ m, we find 25% emittance growth along the linac.

4. FEL PERFORMANCE

The FEL design goal is to produce 10^{14} photons in a subpicosecond pulse for biological imaging. To reach this goal we optimize the FEL for maximum laser power. There are two possible design strategies: a.) large electron energy, in the range of 5 to 10 GeV, and a long undulator to obtain the required FEL power directly at saturation; b.) a lower electron energy, 2 to 3 GeV, with the option of using a tapered wiggler after the SASE saturation, to increase the FEL power further when necessary.

We will investigate both options to optimize the system design. To obtain an initial estimate of the FEL performance and explore the parameter space we have been using the analytical form of the FEL gain obtained by Chin, Kim, and Xie [16]. We have also used a program developed by I. Ben-Zvi and L.-H. Yu [17], and the simulation code TDA [18]. These theories and codes include energy spread, three dimensional effects, and a general betatron focusing. The results are shown in Table 1.

We have considered one case with a high energy beam, option a. This is optimized using the largest undulator parameter, $K=6$, and minimum beam energy, 7 GeV, compatible with a simple undulator design, and an output power larger than 10 GW. The FEL characteristics for this case are given in Table 1, column 2. In the same Table, in column 3, we show the case for a reduced beam energy, and a smaller undulator parameter $K=3.7$. When comparing to the 7 GeV case one should also notice that the betatron wavelength has been reduced as the energy ratio, so that the beam transverse radius is the same in the two cases. Note that at smaller energy the uncorrelated energy spread is larger, affecting the FEL gain, while the correlated component

remains the same. The gain length is shorter at 3.5 GeV than at 7 GeV. The saturated power is lower than in option a, but is still acceptable.

Another possibility is the use of low field, long period undulator, to obtain a large value of the undulator period in a simple electromagnetic structure [19,20,21].

5. UNDULATOR

Our initial discussion of the undulator is done for the parameters given in Table 1, column 2. A simple undulator design can be based on an iron free permanent magnet undulator. For a period of 8.3 cm and a peak magnetic field of 0.78 Tesla, we can select a gap of 1.5 cm. This is a conveniently large gap, that would allow us to install instrumentation for beam diagnostic all along the undulator.

The natural betatron wavelength for a planar undulator with these characteristics is $\lambda_{\beta} = 2^{1/2} \lambda_w \gamma / K = 273$ m. We add additional focusing, to obtain the required betatron wavelength of 62 m, using a FODO type quadrupole system. To obtain the 62m betatron wavelength at 7 GeV we can use 40 cm long quadrupoles separated by 40 cm of drift, with a gradient of 14 T/m. The phase shift per cell is 9° , and the modulation of the betatron wavelength is quite small, with a ratio of maximum to minimum values of only 1.1.

Because of the choice of an iron free undulator the quadrupoles can be placed around the undulator. Their radius is 12 cm, corresponding to a pole tip field of 0.84 Tesla. Having the quadrupoles around the undulator has the advantage that no interruption is required in the undulator itself, avoiding phase matching problems. For the same reason it is possible to position beam steering magnets and other correctors around the undulator in between quadrupoles.

If the selected site at SLAC could contain a 220 m insertion device, one could consider using the weak-field structure discussed in [19-21].

6. X-RAY BEAM LINES AND OPTICS

Extracting and processing the FEL output radiation presents challenging optical engineering problems, because of the unprecedented peak power and brevity of the anticipated radiation pulses. The main tasks will be to: 1) deflect the output radiation out of the bremsstrahlung cone produced by the electrons on the residual gas in the FEL and the upstream collimators; 2) to further monochromatize the radiation, if needed. At the power densities expected at normal incidence, of the order of 10^{16} W/cm², it is easy to assess that energy in excess of 1 eV/atom will be deposited in the irradiated volume and that ablation of the irradiated surface will become probable due to the comparatively long time constants of alternative energy-removal channels. This precludes the use of solid state optics, such as multilayers, that work at large angles of incidence, leaving multi-faceted optics operating at extreme grazing incidence as perhaps the only viable choice.

An alternative approach that could mitigate the damage problem would be to configure a series of gas jets with density gradients.

REFERENCES

1. C Pellegrini, Jour. Opt. Soc. of Amer. B2, 259 (1985).
2. K.-J. Kim et al., Nucl. Instr. and Meth. A239, 54 (1985); K.-J. Kim, Phys. Rev. Letters 57, 1871 (1986); C. Pellegrini, Nucl. Instr. and Meth. A272, 364 (1988); L.-H. Yu and S. Krinsky, Nucl. Instr. and Meth. A285, 119 (1989).

3. R. L. Sheffield, Photocathode RF Guns, in Physics of Particle Accelerators, AIP vol.184, p. 1500, M. Month and M. Dienes eds., (1989).
4. Workshop on Fourth Generation Light Sources, SSRL Report 92/02, M. Cornacchia and H. Winick, editors.
5. C. Pellegrini, *ibid*, p.364.
6. K.-J. Kim, *ibid*. p. 315.
7. W. Barletta, A. Sessler and L. Yu, *ibid*, p. 376-84
8. K. Bane, "Wakefield Effects in a Linear Collider", AIP Conf. Proc., vol. 153, p. 971 (1987).
9. J. Seeman et al, "Summary of Emittance Control in the SLC Linac", US Particle Accelerator Conference, IEEE Conf. Proc. 91CH3038-7, p. 2064 (1991).
10. M. Ross et al, "Wire Scanners for Beam Size and Emittance Measurements at the SLC", US Particle Accelerator Conference, IEEE Conf. Proc. 91CH3038-7, p. 1201 (1991).
11. J. Seeman et al, "Multibunch Energy and Spectrum Control in the SLC High Energy Linac", US Particle Accelerator Conference, IEEE Conf. Proc. 91CH3038-7, p. 3210 (1991).
12. T. Raubenheimer, "The Generation and Acceleration of Low Emittance Flat Beams for Future Linear Colliders", SLAC-Report 387 (1991).
13. J. C. Solem and G. C. Baldwin, Science 218, 229 (1982); M. Howells and J. Kirz, in Free Electron Generation of Extreme UV Coherent Radiation, J. M. J. Madey and C. Pellegrini eds., AIP Vol. 118; p. 85 (1984).
14. K.-J. Kim, Nucl. Instr. and Meth. A275, 201 (1989).
15. C. Hartman and J.B. Rosenzweig, "Ponderomotive Focusing in Axisymmetric RF Linacs", submitted to Phys. Rev. A (1992).
16. Y. H. Chin, K.-J. Kim, and M. Xie, Three Dimensional Free Electron Laser Theory Including Betatron Oscillations, LBL Rep. 32329 (1992), submitted to Phys. Rev. A.
17. I. Ben Zvi and L.-H. Yu, private communication.
18. T.M. Tran and J. S. Wurtele, Comp. Phys. Commun. 54, 263 (1989).
19. R. Tatchyn, "Optimal Insertion Device Parameters for SASE FEL Operation," Workshop on Fourth Generation Light Sources, SSRL Report 92/02, M. Cornacchia and H. Winick. eds., 605(1992).
20. R. Tatchyn, T. Cremer, and P. Csonka, "Design considerations for a new weak-field soft X-ray undulator/FEL driver for PEP," Nucl. Instrum Meth. A308, 152(1991).
21. R. Tatchyn, "Fourth Generation Insertion Devices: New Conceptual Directions, Applications, and Technologies," Workshop on Fourth Generation Light Sources, SSRL Report 92/02, M. Cornacchia and H. Winick. eds., 417(1992).

TABLE 1
FEL CHARACTERISTICS

ELECTRON BEAM PROPERTIES: GUN EXIT	Option A	Option B
Energy, MeV	10	10
Emittance, normalized, rms, mm-mrad	3	3
Pulse duration, rms, ps	1.6	1.6
Relative energy spread, rms, %	0.15	0.15
Peak current, A	250	250
ELECTRON BEAM PROPERTIES: HIGH ENERGY		
Energy, GeV	7	3.5
Emittance, normalized, rms, mm-mrad	3	3
Peak current, A	2,500	2,500
Uncorrelated energy spread, rms, %	0.04	0.07
Correlated energy spread, rms, %	0.1	0.1
UNDULATOR PROPERTIES		
Period, cm	8.3	5
Magnetic field, T	0.78	0.8
Undulator parameter	6	3.7
Betatron wavelength, m	62.8	31.4
FEL PROPERTIES		
Wavelength, nm	4	4
Field gain length, m	6.9	5.3
Undulator saturation Length, m	60	48
Peak power at saturation, GW	28	10
Pulse duration, rms, ps	0.16	0.16
Line width, rms, including chirping, %	0.2	0.2
Photons per pulse	2.7×10^{14}	1×10^{14}
Energy per pulse, mJ	11	4
Peak brightness, Ph/mm ² /mrad ² /s/0.1% ($\Delta\omega/\omega$)	5.3×10^{31}	2.0×10^{31}
Repetition rate, Hz	120	120
Average power, W	1.2	0.5
Average brightness, Ph/mm ² /mrad ² /s/0.1% ($\Delta\omega/\omega$)	1.0×10^{21}	3.7×10^{20}

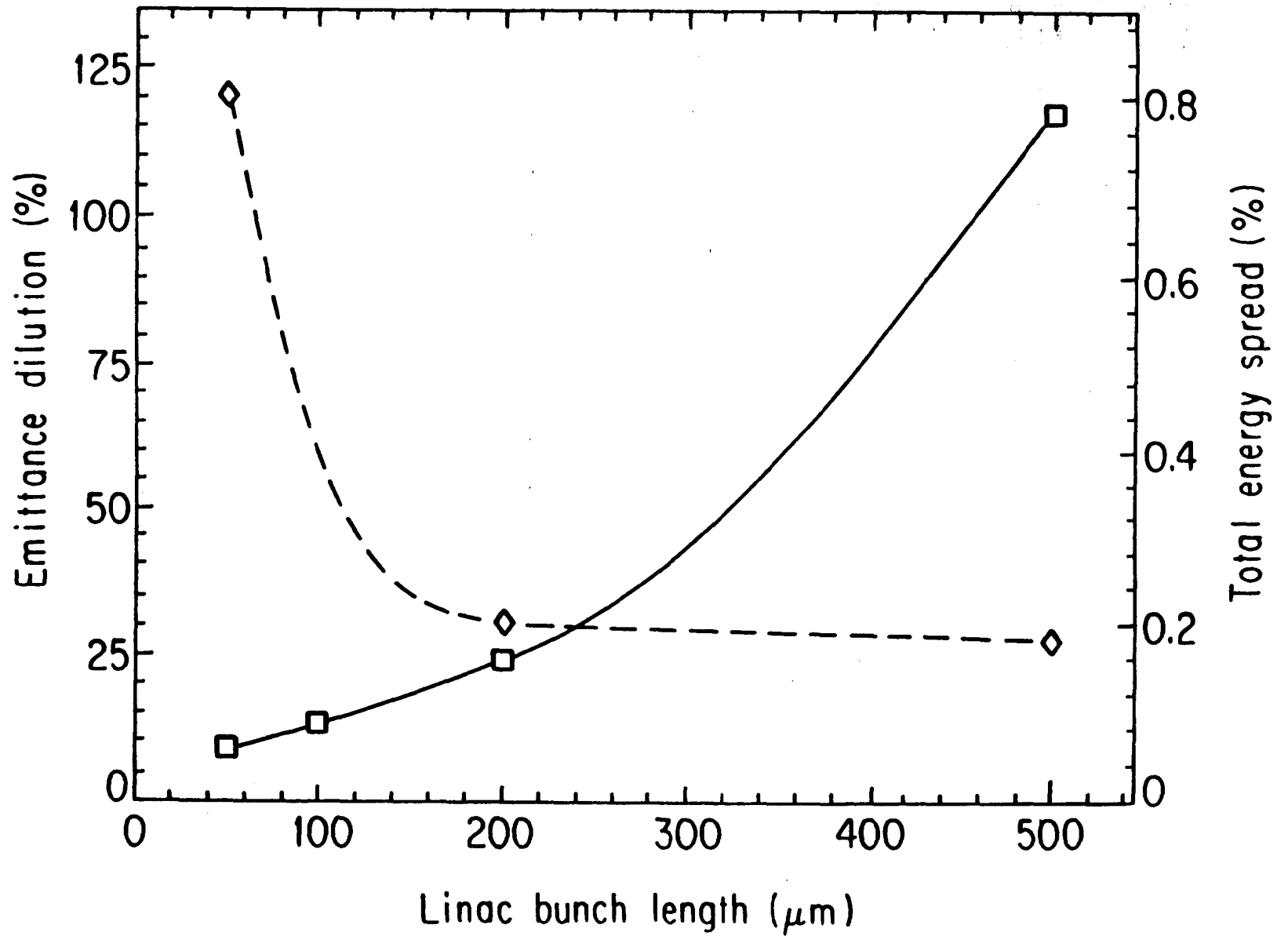


Figure 2 Transverse emittance dilution (solid line) and peak-to-peak energy spread (dashed line) as a function of the bunch length. The points are the values calculated and the lines are for guidance.

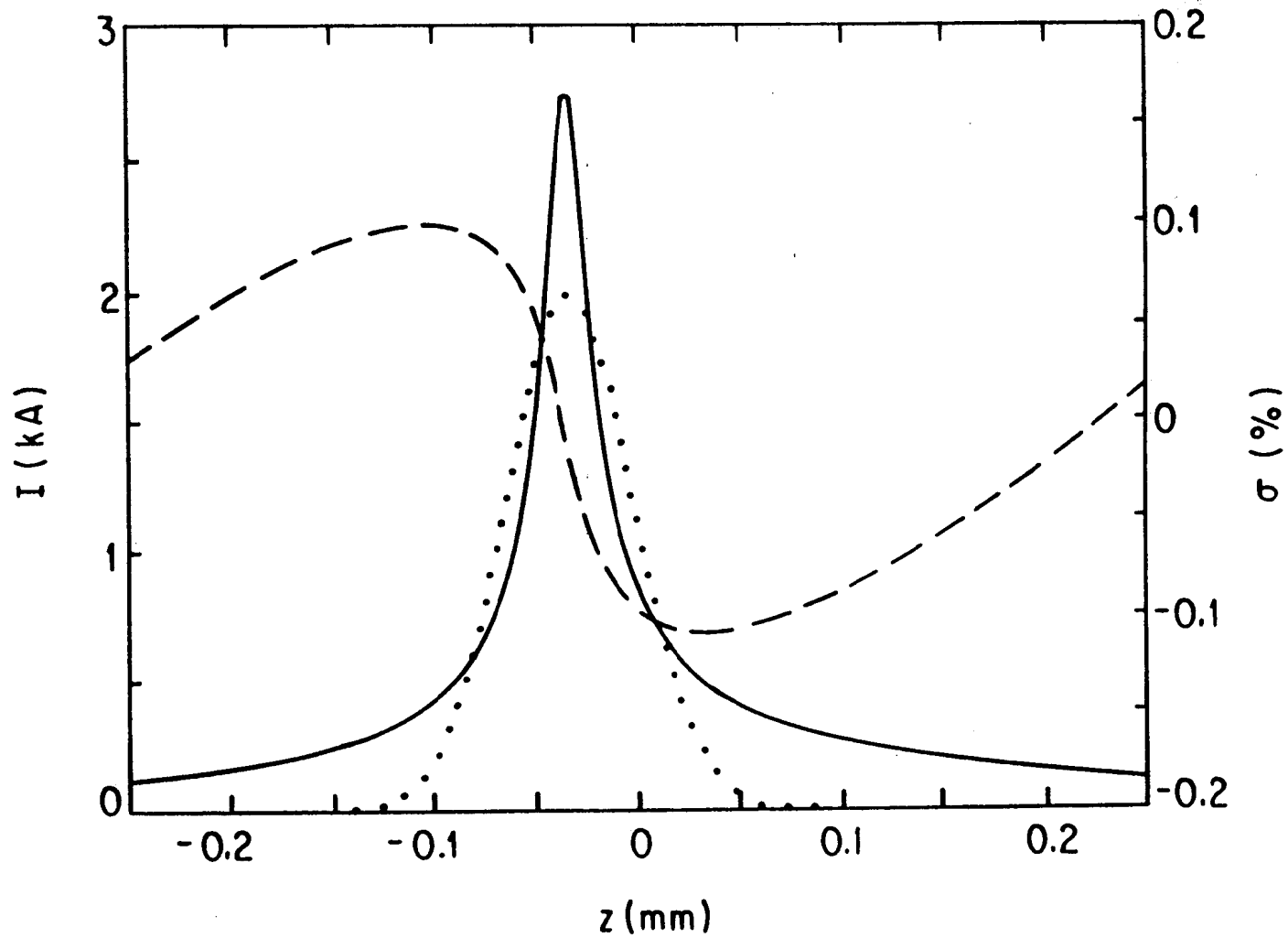


Figure 1 Current distribution after the final compression (solid line) and a gaussian fit to the core (dots); the head of the bunch is to the left. The energy variation correlated with longitudinal position is shown on the right axis; the uncorrelated energy spread is 0.04%.